Electroexcitation of 4^- states in ^{16}O

C. E. Hyde-Wright,[a] W. Bertozzi, T. N. Buti,[b] J. M. Finn,[c] F. W. Hersman,[d] M. V. Hynes,[e] M. A. Kovash,[f] J. J. Kelly,[g] S. Kowalski, J. Lichtenstadt,[h] R. W. Lourie, B. E. Norum,[i] B. Pugh,[f] and C. P. Sargent
Department of Physics, Laboratory for Nuclear Science and Bates Linear Accelerator Center, Massachusetts Institute of Technology, Cambridge, Massachusetts 02139

B. L. Berman
Lawrence Livermore National Laboratory, University of California, Livermore, California 94550 and The George Washington University, Washington, D.C. 20052

F. Petrovich and J. A. Carr[j]
Department of Physics, Florida State University, Tallahassee, Florida 32306
(Received 28 August 1986)

We report electron scattering form factors for known 4^- states in ^{16}O at 17.79 and 18.98 MeV. We also report statistical upper bounds for the 4^- state at 19.80 MeV. The ratios of these form factors are consistent with the isospin amplitudes derived from pion scattering data. The form factors of levels observed in (e,e') at 17.880 ± 0.015, 18.635 ± 0.020, and 20.510 ± 0.025 MeV are compatible with 4^- $T=1$ assignments. Existing (π,π') and (p,p') spectra do not contradict these identifications. The 4^- form factors are well described by a harmonic-oscillator density with oscillator length $b=1.58$ fm. This value is substantially smaller than the value of 1.77 fm obtained from the ground state charge density. The form factor of the 18.98 MeV state can also be fitted by a Woods-Saxon transition density, with parameters fitted to the elastic $M5$ multipole of ^{17}O. The fit is improved by inclusion of meson-exchange currents. However, the isoscalar-isovector differences in the Woods-Saxon plus meson-exchange current form factors result in a poor fit to the 17.79 MeV state. The total isovector and isoscalar strengths observed for the established 4^- states are 41% and 23%, respectively, of a pure single-particle prediction.

I. INTRODUCTION

Three 4^- states have been identified previously in ^{16}O at excitation energies of 17.79, 18.98, and 19.80 MeV. A level near 19 MeV was seen in electron scattering by Sick *et al.*,[1] and identified as an isovector 4^- state. In a comparison of $^{17}O(d,t)^{16}O$ and $^{17}O(d,^3He)^{16}N$ spectra,[2] the 18.98 MeV state was again identified as an isovector 4^- level and the other two states were identified as isoscalar 4^- levels. This triad of states was also observed in 135 MeV proton scattering[3] and 164 MeV pion scattering.[4] We report electron scattering cross sections for the 4^- $T=0$ state at 17.79 MeV and the 4^- $T=1$ state at 18.98 MeV. We also report statistical upper bounds for the 4^- $T=0$ state at 19.80 MeV. In addition, we have measured the electromagnetic form factors of narrow states at 17.880 ± 0.015 MeV, 18.635 ± 0.020, MeV, and 20.510 ± 0.025 MeV. These form factors are purely transverse, indicating abnormal parity assignments. The momentum transfer dependence of these transitions is very similar to the form factors measured for the known 4^- states, suggesting 4^- spin-parity assignments.

In the shell model, 4^- states have maximal angular momentum for the excitation of a nucleon from the $1p$ shell to the $2s$-$1d$ shell. Such "stretched" states provide important tests for the nuclear shell model and for intermediate energy reaction models. In the model discussed in Refs. 5—7, electron, pion, and nucleon scattering are related through a common spin transition density. Within the precision of the analyses, the relative excitation strengths of the 4^- states at 17.79, 18.98, and 19.80 MeV, as measured by electron scattering, are consistent with the isospin-mixing amplitudes derived from analyses of pion scattering data for these same transitions.[4,8,9] The (π,π') analyses determine the relative strengths of the 4^- levels. Our electron scattering data determine the absolute magnitude and shape of the transition densities. Based on these densities, distorted-wave impulse approximation (DWIA) calculations are consistent to within 20% in absolute magnitude to the intermediate energy (π,π') cross sections.

The electron scattering $M4$ form factors are strongly enhanced at high q relative to a harmonic-oscillator calculation based on the ground state properties of ^{16}O. This enhancement can be explained only partially by meson exchange currents (MEC)'s. The enhancement can be parametrized as a shrinking of the radial scale of the single particle orbits for the 4^- states relative to the ground state. Such a shift is compatible with the Woods-Saxon parameters fitted to the ^{17}O elastic $M5$ form factor.

II. ELECTRON SCATTERING EXPERIMENT AND ANALYSIS

The electron scattering cross section for the excitation of a discrete state is given in plane wave Born approximation (PWBA) by[10]

$$\frac{d\sigma}{d\Omega}=Z^2\sigma_{\text{Mott}}\frac{1}{\eta}\left[\frac{q_\mu^4}{\mathbf{q}^4}|F_L(\mathbf{q}^2)|^2+\left[\frac{|q_\mu^2|}{2\mathbf{q}^2}+\tan^2\frac{\theta}{2}\right]|F_T(\mathbf{q}^2)|^2\right],$$
$$\sigma_{\text{Mott}}=\frac{\alpha^2\cos^2(\theta/2)}{4E_1^2\sin^4(\theta/2)},\quad \eta=1+2\frac{E_1}{M_T}\sin^2(\theta/2)\ . \tag{1}$$

In Eq. (1), θ is the scattering angle, E_1 is the incident electron energy, and $q_\mu=(\omega,\mathbf{q})$ is the four-momentum transfer. For an abnormal-parity transition, $F_L(\mathbf{q}^2)\equiv 0$. The static Coulomb field of the nucleus introduces distortions to the incoming and outgoing partial waves. For a low-Z target such as ^{16}O, this effect can be accounted for by defining the experimental form factor as a function of the effective momentum transfer:[11]

$$q_{\text{eff}}=|\mathbf{q}|[1+eV_C(r)/E_1]\ . \tag{2}$$

In Eq. (2), $V_C(r)$ is the Coulomb field of the nucleus, evaluated at the Bessel function maximum: $r=(l+1)/|\mathbf{q}|$, where l is the minimum orbital angular momentum transfer for a particular transition. We approximate V_C using the Coulomb field of a uniform charge density with root mean square radius equal to 2.72 fm—the experimental value for ^{16}O (Ref. 12).

This experiment was performed at the Bates Linear Accelerator Center, using the Energy Loss Spectrometer System (ELSSY). The measurements were made at laboratory scattering angles of 90°, 140°, and 160° and span a momentum transfer range of 1.0—2.5 fm^{-1}. Natural beryllium oxide foils were used with thickness ranging from 20 to 40 mg/cm^2. The targets were oriented in transmission mode, with the normal to the target bisecting the scattering angle. The spectrometer aperture was ± 13.1 mr in the scattering plane and ± 63.5 mr in the spectrometer bend plane. Details of the dispersion-matched beam transport and spectrometer system can be found in Ref. 13. The focal-plane instrumentation is described in Ref. 14. The resolution was generally limited by the target thickness, and ranged from 40 to 100 keV full width at half maximum (FWHM). Sample fitted BeO(e,e') and Be(e,e') spectra are shown in Fig. 1.

Cross sections were extracted from the spectra with the line shape program ALLFIT.[15,16] The total function fitted to the BeO spectrum in Fig. 1 consists of three contributions: (1) An "^{16}O continuum" curve which describes the ^{16}O continuum and the tails of peaks lying outside the spectrum. This curve is a piecewise polynomial with a discontinuity in the slope and curvature at a specific threshold. This threshold generally was set to the ^{16}O neutron-decay threshold of 15.66 MeV. In Fig. 1 this threshold is set to the ^{16}O proton-decay threshold at 12.13 MeV, but the contribution of the ^{16}O continuum becomes important only above the neutron decay threshold. (2) A "^{9}Be continuum" curve derived from the ^{9}Be(e,e') spectrum obtained under the same kinematics. Line shape analysis was used to subtract the discrete ^{9}Be peaks from the ^{9}Be(e,e') spectrum. The resulting experimental continuum spectrum then was smoothed to obtain the curve in

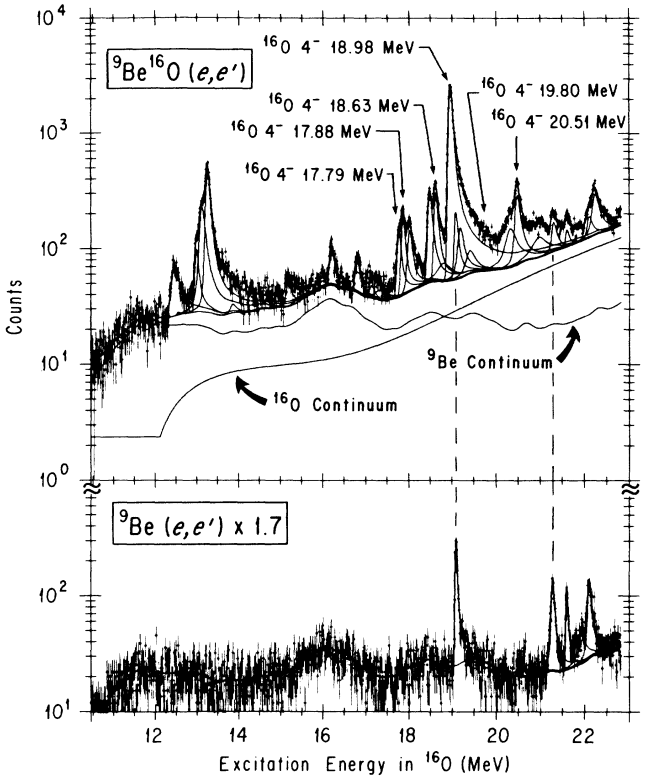

FIG. 1. Fitted ^{9}Be^{16}O(e,e') (top) and matching ^{9}Be(e,e') (bottom) spectra. The spectra were obtained for $E_1=230$ MeV and $\theta=160°$. The six states in ^{16}O which are the subject of this paper are indicated. See text for explanation of curves. The ^{9}Be data and curves in the bottom figure have been multiplied by 1.7 to match the contribution of Be to the BeO spectrum in the top figure. This factor of 1.7 accounts for the differences in the ^{9}Be areal density, the integrated beam charge, and the dead time correction for the two spectra. The prominent peaks in the ^{9}Be spectrum are at 14.39, 16.67, 16.98, and 17.49 MeV in ^{9}Be. The ripples in the ^{9}Be continuum curve are not statistically significant.

Fig. 1. The statistical uncertainty in the smoothed curve was propagated into the extracted ^{16}O cross sections. (3) A line shape for each quasidiscrete state in ^{16}O and ^{9}Be. The line shapes for the ^{9}Be peaks in the BeO spectra generally were constrained to yield the cross sections obtained from ^{9}Be(e,e') spectra. The line shape for each state is a convolution of three contributions: (a) the intrinsic resolution function of the experiment, (b) the radiative response function, and (c) a Lorentzian excitation function for states with decay widths greater than 5 keV. Because these measurements were made above the ^{16}O hadronic decay threshold, the distinction between a δ function, a Gaussian, or a Lorentzian shape in (c) has an important effect on the integrated cross section of a given level. A nuclear level in the continuum has a tail which is best described by the Lorentzian shape.

The BeO spectrum in Fig. 1 contains plots of the total fitting function and each of the continuum curves described above. In addition, a curve is plotted for each

state. This curve is the sum of the line shape of the state and the ^{16}O and ^{9}Be background curves (1) and (2). For the ^{9}Be spectrum, the smoothed continuum curve and the contributions of each discrete peak are plotted.

The primary challenge posed by the analysis was to determine the number of states present in the spectra, and their excitation energies and decay widths. In brief, the states in Table I were identified from the systematics of our (e,e′) data and from supplementary information from the literature,[1–4,17–26] particularly the compilation of Ref. 27. A detailed discussion of our complete results spanning the excitation region from 12 to 22 MeV was the subject of a Ph.D. thesis[28] and will be presented in a forthcoming paper. The parameters in Table I are a minimal choice which fit our data. The broad states may be the sum of several narrower states. With the exception of the levels at 18.3, 19.80, and 20.2 MeV, every level in Table I is explicitly included in the fit in Fig. 1. The broad levels at 18.3 and 20.2 MeV were significant only for $q \leq 1.5$ fm^{-1}. The state at 19.2 MeV was identified primarily by its strength in our 90° spectra. The level at 19.4 MeV was identified from the (e,e′) systematics and from proton scattering spectra obtained at the Indiana University Cyclotron Facility (IUCF).[29] A compilation of the data for the six states which are the focus of this paper (Figs. 1–3) is available from PAPS.[30]

Electron scattering measurements in this region of ^{16}O have been published by a number of authors. The measurements of Sick *et al.*[1] span the range of momentum transfer from 0.4 to 3.0 fm^{-1}, which overlaps the present experiment. Additional electron scattering data, confined to momentum transfers of less than 1 fm^{-1}, are reported in Refs. 17–21. Graves *et al.*[22] summarized these earlier (e,e′) experiments, which typically were performed with low resolution. Recently, Küchler *et al.*[23] measured levels in ^{16}O from 16 to 20 MeV with excellent resolution for momentum transfers from 0.3 to 0.5 fm^{-1}. Single nucleon transfer,[2] proton scattering,[3] and pion scattering[4] measurements of 4^- states in ^{16}O were already mentioned above. Kemper *et al.*,[24] Nann *et al.*,[25] and Hamill *et al.*[26] measured levels in mass 16 via three particle transfer reactions. Some salient features of these references pertinent to the assignment and structure of 4^- levels are given in the next section.

TABLE I. ^{16}O levels observed in this work between 17.7 and 20.7 MeV. All excitation energies, widths, spins, parities, and isospins are from Ref. 27, except where otherwise noted. Values in parentheses are tentative assignments from this work.

E_x (MeV)	$J^\pi;T$	Γ (keV)	Γ^a (keV)
17.788±0.016	$4^-;0$	150±60	20±20
17.880±0.015[a]	$(4^-;1)$		20±20
18.033±0.010	$3^-;1$	26± 5	
≈18.3[a]			≈430
18.500±0.010[b]	$2^-;1$	60±10	35±15
18.635±0.020[a]	$(4^-;1)$		35±30
≈18.8			320±140
18.975±0.010	$4^-;1$	<40	10±10
19.206±0.012	$3^-;1$	68±10	
19.430±0.020[a]			150±15
19.802±0.016[c]	$4^-;0$	36± 5	
20.185±0.040[a]			400±100
20.335±0.025[a]			≈200
20.510±0.025[a]	$(4^-;1)$		50±30

[a]This work
[b]E_x, J^π, T, and Γ from Ref. 23.
[c]Not observed in this work.

III. SPECTROSCOPY OF 4^- STATES IN ^{16}O

A. Level assignments

The transverse form factors for the 17.79 and 18.98 MeV states observed in this work are plotted in Fig. 2. The state at 19.80 MeV was not observed; consequently, only statistical upper bounds were extracted. We fitted the data with a harmonic oscillator $[1d_{5/2} \otimes 1p_{3/2}^{-1}]_{4^-}$ transition density. The oscillator length b and spectroscopic amplitudes Z_T (defined in Ref. 31) were adjusted to fit the data, assuming spectroscopic purity for each state. The nucleon and center-of-mass form factors are included as explicit factors in the fitting function. The parameters obtained are given at the top of Table II. The results are shown in Fig. 2. Although the oscillator lengths obtained for the 17.79 and 18.98 MeV states differ slightly, the spectroscopic amplitude of the 17.79 MeV state is insensitive to this difference. The two fits to the

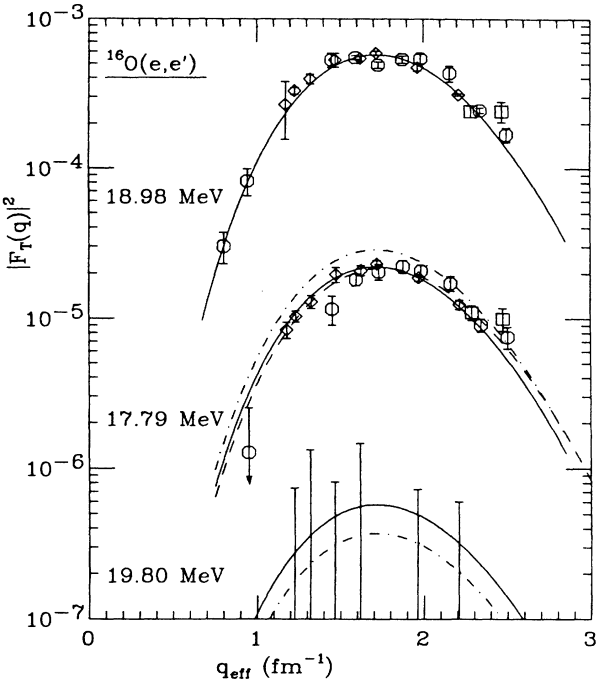

FIG. 2. Transverse form factors of established 4^- states in ^{16}O. Octagon, 90°; diamond, 160°; square, 140°. The curves are harmonic-oscillator calculations. Solid, fit with $b=1.58$ fm, Table II; dashed, $b=1.54$ fm, Table II; dotted-dashed, $b=1.58$ fm, Table III, DWIA. For the 19.80 MeV state the data are statistical upper bounds obtained at 160°.

TABLE II. Parameters for harmonic-oscillator fits of 4⁻ states. Values without error bars were not varied.

State (MeV)	b (fm)	$Z_{T=0}$	$Z_{T=1}$	χ_ν^{2b}
17.79	1.54±0.01	0.65±0.01	0.0	1.1
17.79	1.58	0.66±0.01	0.0	1.7
18.98	1.58±0.01	0.0	0.63±0.01	2.4
19.80	1.58	≤0.1[a]	0.0	
17.88	1.58	0.0	0.15±0.002	5.8
18.63	1.58	0.0	0.18±0.002	6.0
20.51	1.58	0.0	0.23±0.002	5.5

[a]One standard deviation upper bound.
[b]χ^2 per degree of freedom.

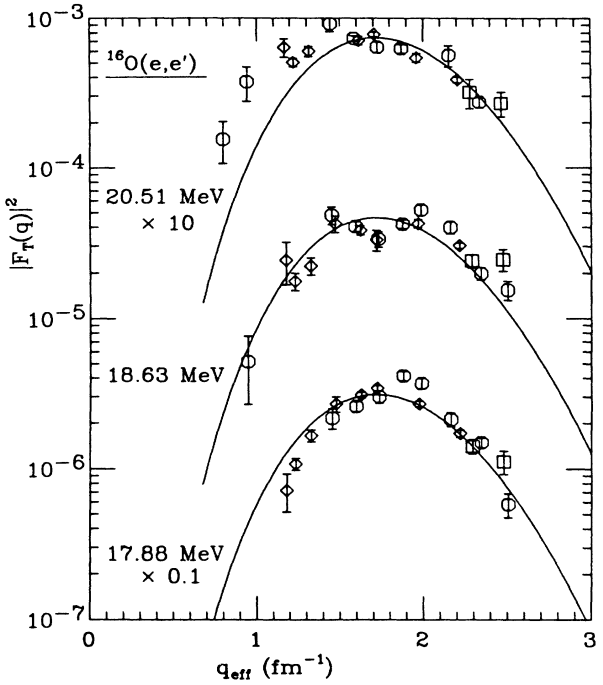

FIG. 3. Transverse form factors squared for new 4⁻ states in ^{16}O. The data are plotted assuming the longitudinal form factor vanishes. The data symbols are the same as Fig. 2. The curves are the harmonic-oscillator $M4$ fits of Table II.

17.79 MeV state set the scale for any isospin dependence to the ($\Delta L=3$, $\Delta S=1$) spin flip density. The oscillator constant $b=1.58$ obtained in these fits is in striking contrast to the value 1.8 fm generally accepted for ^{16}O. This contrast will be discussed more completely in Sec. IV.

Among the new states observed in this experiment, the three states at 17.88, 18.63, and 20.51 MeV have purely transverse form factors with shapes that are similar to those of the 4⁻ states. These states are listed in Table I and displayed in Fig. 3. The degree of consistency between the data at 90°, 160°, and 140° determines the level of confidence in the abnormal parity assignment. The curves in Fig. 3 are the same harmonic oscillator fits as in Fig. 2, with the isovector amplitudes adjusted to fit each state. The amplitudes are tabulated at the bottom of Table II. The most probable alternative assignment for any of these states is 2⁻. The $M2$ mode in ^{16}O has many degrees of freedom—five independent $[(2s1d)^1 \otimes 1p^{-1}]_{2^-}$ configurations.

Sick *et al.*[1] observed a strong peak in ^{16}O(e,e') near 19.0 MeV. This was attributed to the isovector 4⁻ shell-model state with additional contributions from 2⁻ $T=1$ levels. The resolution was several hundred keV, but results were quoted only for cross sections integrated over a 1 MeV bin. The transverse form factor squared for the "20 MeV complex" plotted in Fig. 3(a) of Ref. 1 is roughly a factor of 2 larger than the data reported here for the isovector 4⁻. This factor of 2 is consistent with the present data. For example, in our 160° data at $q=1.6$ fm^{-1} (the peak of the form factor) the 18.98 MeV 4⁻ state accounts for only 65% of the strength observed above the background continuum between 18.5 and 19.5 MeV. The remaining 35% of the strength is shared by the other states listed in Table I.

Küchler *et al.*[23] report 2⁻ levels at 17.78, 18.50, and 19.0 MeV (±0.01 MeV). The level at 19.0 MeV is part of a broad concentration of strength distributed between 18.7 and 19.4 MeV. A similar distribution was observed underlying the 18.98 MeV 4⁻ peak in the present work. The 18.50 MeV peak is also apparent in our data. Low momentum transfer electron scattering is primarily sensitive to low multipolarity transitions. The fact that the 18.63 and 17.88 MeV levels were not observed in Ref. 23 can be taken as evidence for the high spin assignment suggested here. The observed strength at 17.79 MeV presents more of a problem, but is consistent with the existence of nearly degenerate 2⁻ and 4⁻ levels: If the harmonic oscillator fit to the 17.79 MeV level of Fig. 2 is extrapolated to momentum transfers less than 0.5 fm^{-1}, the extrapolated $|F_T(q)|^2$ lies more than two orders of magnitude below the data that Küchler *et al.* report for a 2⁻ level at 17.78±0.01 MeV. Similarly, a 2⁻ form factor is likely to be negligible relative to the 4⁻ factor at the high momentum transfers of this experiment. The large strength observed for the 17.79 MeV state at high q in intermediate energy pion and proton scattering conclusively identifies a stretched 4⁻ state at this energy.

The transverse (e,e') strength of the states we observed at 17.88, 18.63, and 20.51 MeV is roughly one-tenth that of the isovector 4⁻ state at 18.98 MeV, and twice that of the 17.79 MeV isoscalar 4⁻ state. If any of these new states were predominantly isoscalar 4⁻ levels, then their (e,e') strength would imply one-particle one-hole (1p1h) spectroscopic amplitudes of nearly unity. This, in turn, would require these states to have larger cross sections than the known 4⁻ states in intermediate energy hadron scattering, which is not observed.[3,4,29] Thus an isoscalar 4⁻ assignment can be excluded. On the other hand, an isovector 4⁻ assignment to any of these states implies that the cross sections for each of these states in intermediate energy hadron scattering would be in the same 1:10 ratio to the 18.98 MeV state as they are in (e,e'). The pion

scattering spectrum in Fig. 1 of Holtkamp *et al.*[4] does not exclude the presence of levels at 18.63 and 20.51 MeV with the prescribed factor of 10 reduction in strength from the 18.98 MeV level. The 17.88 MeV level, if present, is not resolved from the 17.79 MeV level. The 4^- states at 17.79, 18.98, and 19.80 MeV are strongly excited in proton scattering on ^{16}O at proton kinetic energies of 135 and 180 MeV.[3,29] In addition, states at 18.6 and 20.5 MeV are observed in the spectra with strength roughly one-tenth of the 18.98 MeV level.[29] Analysis of the (p,p') peak at 17.79 MeV does not show a broadening due to a strong level at 17.88 MeV.[29] Bearing in mind the consistency of the peak position observed at 17.79 MeV in (e,e'), (π,π'), and ^{17}O(d,^{3}H), we conclude that the existing data are compatible with the assignments for the three states at 17.88, 18.63, and 20.51 MeV to be 4^- isovector states. These 4^- assignments also imply that each state is dominated by multiparticle, multihole excitations of the ^{16}O ground state, with only a small 1p1h 4^- amplitude.

Additional evidence regarding the 18.63 and 20.51 MeV states is obtained from three-particle three-hole (3p3h) transfer reactions. Kemper *et al.*[24] measured the ^{13}C(^{6}Li,^{3}H)^{16}O spectrum and found the strongest state to be at 20.57±0.02 MeV. Though there is a small discrepancy in energy, this could be the same state as the level reported here at 20.510±0.025 MeV. A weaker, though still prominent level, is seen at 18.65 MeV in Ref. 24. States with much less strength are also observed at 17.79, 17.90, 18.98, and 19.80 MeV. Similar results in the range from 18.0 to 19.6 MeV were obtained by Nann *et al.*[25] These data qualitatively support the picture [also seen in ^{14}C (Ref. 32)] of 4^- states with both 1p1h and 3p3h components. The established 4^- states at 17.79, 18.98, and 19.80 MeV have strong 1p1h and weaker 3p3h amplitudes. For the 18.63 and 20.51 MeV levels the 3p3h amplitudes predominate. The weakness of the 17.90 MeV level in the ^{13}C(^{6}Li,^{3}H)^{16}O reaction (Ref. 24) favors a 2^- 1p1h over a 4^- 3p3h assignment. Hammill *et al.*[26] measured 3p3h states in ^{26}N via the ^{13}C(α,p) reaction. The 6.18 MeV analog in ^{16}N of the 18.98 MeV 4^- state in ^{16}O is weakly excited. A strongly excited level at 7.64 MeV was assigned a 3p3h 4^- structure. This is likely the analog of the 20.51 MeV level in ^{16}O. Another strongly excited level at 5.73 MeV was assigned a 2p2h 5^+ structure. This could be the analog of the 18.63 MeV level in ^{16}O. Kemper *et al.*[24] also suggest a 5^+ assignment for this level. In summary, 3p3h transfer reactions support high spin assignments for levels in ^{16}O at 18.63 and 20.57 MeV. More work is required to make exact spin-parity assignments.

B. Isospin mixing

We have shown that the (e,e') strength of the 4^- states at 17.79 and 18.98 MeV are compatible with pure $T=0$ and 1 assignments, respectively, and with equal suppression factors of 0.4 in the squared amplitude. However, electron scattering data cannot uniquely determine the isospin structure of these states. In fact, recent (π,π') data[4] suggest a different picture involving isospin mixing between these states. In the following discussion we summarize the pion scattering analysis, and show how the electron scattering data substantiates the pion analyses.

Pion scattering data for 4^- states in ^{16}O are displayed in Fig. 2 of Ref. 4. Holtkamp *et al.*[4] analyzed the $\pi^\pm$ asymmetries in terms of the Δ-dominance model to extract isospin-mixing amplitudes and matrix elements of the isospin-violating Hamiltonian for the three states at 17.79, 18.98, and 19.8 MeV. The extracted isospin-violating matrix elements may be sensitive to the assumption of a three-state mixing model. However, the analysis of the spectroscopic amplitudes is general and is not affected by the presence of additional 4^- states in the spectrum.

In the Δ-dominance model, inelastic pion scattering from nuclei at pion energies near the Δ resonance is dominated by the process

$$\pi+\mathrm{N}\rightarrow\Delta\rightarrow\pi+\mathrm{N}\ . \tag{3}$$

The incident pion is absorbed on a single nucleon, forming a resonant Δ which then decays into a nucleon plus the outgoing pion. The existence of a unique transition density for stretched particle-hole states means that the relative strengths of $\pi^\pm$ excitation of isoscalar and isovector configurations are given simply by ratios of isospin Clebsch-Gordan coefficients. Let $A_\pm$ denote the $\pi^\pm$ amplitudes for the excitation of a 4^- state in ^{16}O with isoscalar and isovector spectroscopic amplitudes Z_0 and Z_1, respectively. In the Δ-dominance model,[4]

$$\frac{A_+}{A_-}=\frac{2.0Z_0+Z_1}{2.0Z_0-Z_1}\ . \tag{4}$$

A positive admixture of an isovector 1p1h component into a dominantly isoscalar 1p1h state will enhance the π^+ and diminish the π^- scattering, as observed for the 17.79 MeV state. Equation (4) also applies to ratios between states, since the postulated reaction mechanism is common to all 4^- states. For example,

$$\frac{A_+(17.79\ \mathrm{MeV})}{A_+(18.98\ \mathrm{MeV})}=\frac{[2.0Z_0+Z_1]_{17.79\ \mathrm{MeV}}}{[2.0Z_0+Z_1]_{18.98\ \mathrm{MeV}}}\ . \tag{5}$$

The ratios of cross sections are given by the squares of Eqs. (4) and (5). In Ref. 4 the spectroscopic amplitudes were fitted to the ratios of the integrated pion-scattering cross sections for each state (see Table III, heading Δ dominance). This relative analysis leaves the Z_1(18.98 MeV) amplitude undetermined.

The analysis of the pion scattering data was refined by Carr *et al.*,[8] who calculated absolute pion cross sections and angular distributions in the DWIA. The basic variables in their calculation are the nuclear transition density and the pion-nucleon t matrix. Preliminary (e,e') results from the present work for the 18.98 MeV state were used to determine the transition density. The harmonic oscillator form was used with parameters $b=1.62$ fm and $Z_1=0.62$. These values do not differ significantly from the final values quoted here. The π-N transition operator used was the p-wave form of the spin-orbit operator, adjusted to fit free π-N scattering data. In Ref. 8 agreement was obtained between the DWIA calculation and the relative magnitude of the six (π,π') angular distributions by

adjusting the relative isospin-mixing amplitudes of the three 4^- states. The absolute magnitude of the calculated (π,π') cross sections is fixed by the spectroscopic amplitude of the 18.98 MeV state, taken from the present work. The authors of Ref. 8 applied a uniform adjustment of 1.15 to the pion-nucleon t matrix to fit the DWIA calculation to the (π,π') data. This adjustment to the t matrix sets the scale for the absolute accuracy of the DWIA calculation. The isospin-mixing amplitudes are displayed in Table III under the heading DWIA. These differ only slightly from the results obtained with the Δ-dominance model. Angular distributions, rather than the integrated cross sections, were fitted. By including all p-wave channels in the t matrix, not just the dominant (3,3) resonance, the DWIA requires 1.9 instead of 2.0 in Eq. (4). In addition, the DWIA produces a small π^+/π^- asymmetry from distortion effects.

The Δ-hole model also has been applied[9] to the case of stretched particle-hole transitions in ^{16}O. In addition to the impulse approximation amplitude [Fig. 4(a)], the Δ-nucleon interaction can excite the 4^- particle-hole pair, as in Fig. 4(b). Karapiperis and Moniz[9] assume the Δ-N interaction is dominated by the $\Delta N \rightarrow NN$ annihilation channel. This assumption constrains the ΔN pair to have $T=1$. Let Z'_T denote the spectroscopic amplitudes derived from the data in the Δ-hole mode and let $\mathscr{A}_a$ and $\mathscr{A}_b$ denote the isospin reduced amplitudes corresponding to the diagrams in Figs. 4(a) and 4(b), respectively. Then,[9]

$$\frac{A_+}{A_-}=\frac{2Z'_0(\mathscr{A}_a+\frac{3}{4}\mathscr{A}_b)+Z'_1(\mathscr{A}_a-\frac{5}{4}\mathscr{A}_b)}{2Z'_0(\mathscr{A}_a+\frac{3}{4}\mathscr{A}_b)-Z'_1(\mathscr{A}_a-\frac{5}{4}\mathscr{A}_b)} . \quad (6)$$

Equation (6) reduces to the Δ-dominance expression if $\mathscr{A}_b=0$. The authors of Ref. 9 estimate $\mathscr{A}_b/\mathscr{A}_b=-0.08$ fitting by Eq. (6) to the $\pi^\pm$ ratio for quasielastic proton knockout, which they assume is a pure particle-hole final state. Since $|A_+/A_-|^2$ is an experimental ratio, Eqs. (6) and (4) can be equated. This generates an expression for the primed coefficients (Δ-hole analysis) in terms of the unprimed values (Δ-dominance analysis) for a given transition

$$\frac{Z'_1}{Z'_0}=\frac{Z_1}{Z_0}\frac{1+\frac{3}{4}(\mathscr{A}_b/\mathscr{A}_a)}{1-\frac{5}{4}(\mathscr{A}_b/\mathscr{A}_b)}=0.85\frac{Z_1}{Z_0} . \quad (7)$$

The analysis in Ref. 9 was applied only to extract the Z'_0/Z'_1 ratio for each 4^- state. However, the analysis can be extended to determine the ratios of spectroscopic amplitudes for pairs of 4^- states. For example,

$$\frac{A_+(17.79\text{ MeV})}{A_+(18.98\text{ MeV})}=\frac{[(2Z'_0+Z'_1)\mathscr{A}_a+\frac{1}{4}(6Z'_0-5Z'_1)\mathscr{A}_b]_{17.79\text{ MeV}}}{[(2Z'_0+Z'_1)\mathscr{A}_a+\frac{1}{4}(6Z'_0-5Z'_1)\mathscr{A}_b]_{18.98\text{ MeV}}} . \quad (8)$$

All of the $M4$ transitions are assumed to be dominated by the same stretched particle-hole structure Thus the amplitudes $\mathscr{A}_{a,b}$ are state independent. From Eq. (6) and from the experimental results for the 18.98 MeV level that $|A_+/A_-|^2=1$ (Ref. 4) and $Z_1\neq 0$ (Ref. 2), we conclude that $Z'_0=Z_0=0$ for this level. Z_1(18.98 MeV) is fixed by the present electron scattering data, independent of the pion scattering analysis. Simplifying Eq. (8), equating it with Eq. (5), and applying Eq. (7) gives

$$Z'_1(17.79\text{ MeV})=Z_1(17.79\text{ MeV}) . \quad (9)$$

The same result applies for the state at 19.80 MeV. Equations (7) and (9) summarize the Δ-hole model results, which alter the isoscalar, but not the isovector, amplitudes of the two predominantly isoscalar 4^- states. This is shown in Table III, under the leading Δ hole.

These analyses of the pion scattering data predict the

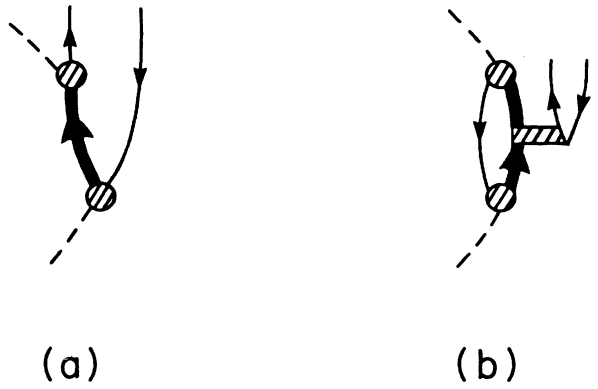

FIG. 4. Diagrams for pion scattering excitation of a particle hole state in the Δ-hole formalism (Ref. 9): (a) impulse approximation and (b) Δ rescattering excitation of particle-hole pair.

TABLE III. Spectroscopic amplitudes from combined electron- and pion-scattering analyses. All amplitudes are fitted relative to Z_1 (18.98 MeV). Z_1 (18.98 MeV) is obtained from the (e,e') analysis. Error bars include (π,π') statistical uncertainty only.

State (MeV)		Δ dominance	$(\pi^\pm,\pi^{\pm\prime})$ analysis DWIA	Δ hole
17.79	Z_0	0.32±0.03	0.33±0.03	0.37±0.04
	Z_1	0.079±0.013	0.077±0.013	0.079±0.04
18.98	Z_0	0.001±0.011	0.001±0.011	0.0
	Z_1	0.63	0.62	0.63
19.80	Z_0	0.34±0.03	0.35±0.03	0.39±0.03
	Z_1	−0.078±0.013	−0.075±0.013	−0.078±0.013

relative strengths for the electron scattering excitation of these states. Specifically, if $A_{(e,e')}$ denotes the electron scattering amplitude analogous to $A_{\pm}$, then

$$\frac{A_{(e,e')}(17.79\ \text{MeV})}{A_{(e,e')}(18.98\ \text{MeV})}=\frac{Z_0\mu_0+Z_1\mu_1}{Z_1\mu_1}\ , \tag{10}$$

where μ_0 and μ_1 denote the nucleon isoscalar and isovector magnetic moments, respectively, and $\mu_1/\mu_0=5.35$. The predicted ratios for the (e,e') form factors squares are compared with the electron scattering data in Table IV. The predicted form factors for the 17.79 and 19.80 MeV states (relative to the 18.98 MeV state) are plotted in Fig. 2. For the 19.80 state, the predicted bound from Eq. (10) is plotted. It is important to note that according to this analysis, the isoscalar amplitudes of the 17.79 and 19.80 MeV states are roughly equal. For electron scattering, the isovector and isoscalar scattering amplitudes contribute approximately equally to the observed form factors of these states. For the 17.79 MeV state, the interference between these two amplitudes is constructive, whereas for the 19.80 MeV state the interference is destructive. Figure 19 of Ref. 7, which is based on preliminary data from this experiment, shows this isospin interference effect explicitly.

IV. THE $M4$ TRANSITION DENSITY

A. Radial wave functions

In a shell model description of ^{16}O limited to the $1p$ and $2s$-$1d$ shells, the $M4$ form factors are pure $[1d_{5/2}\otimes 1p_{3/2}^{-1}]_{4^-}$ densities. We have already shown that the (e,e') data are well described by such a $1\hbar\omega$ configuration, but with a reduced intensity and an anomalously small radial scale. If the dynamics of ^{16}O excite orbitals above the $2s\,1d$ shell, then new degrees of freedom will be added to the $1\hbar\omega$ 4^- form factor. Furthermore, the fractionation and suppression of $M4$ strength implies strong mixing of the $1\hbar\omega$ amplitude with either multiparticle multihole configurations or multi-$\hbar\omega$ 1p1h configurations.

However, we do not have an adequate theoretical description of the dynamics beyond $1\hbar\omega$. For example, Dubach[33] has carried out a shell-model calculation in a space including all orbitals from the $1s$ shell to the $3s\,2d\,1g$ shell, All 2p2h configurations are included in the ground state, and up to 3p3h configurations are included in the negative-parity states. The Hamiltonian is derived from a combination of the interactions in Refs. 34—36. In spite of the large shell-model space, the calculation differs only slightly from the results obtained for 4^- states in a 1p1h space. One isovector and one isoscalar 4^- state are predicted at 20.78 and 20.25 MeV, respectively. For each state, a value of 0.97 is obtained for the $[1d_{5/2}\otimes 1p_{3/2}^{-1}]_{4^-}$ spectroscopic amplitude. The next largest amplitude for any other configuration has a value of 0.02. The calculation fails to predict the suppression of either the isoscalar or isovector $M4$ strength. Nor does the calculation produce the splitting of isoscalar strength into two equal states.

In the absence of a better theoretical framework, we continue to describe the stretched states purely in terms of the $1\hbar\omega$ degrees of freedom. Shell-model calculations do not determine the single-particle wave functions. We rely on phenomenological constraints to suggest the proper form of the orbitals. In Fig. 5 we plot the 375 MeV ^{16}O elastic electron scattering data of Sick and McCarthy.[37] The data are compared with a distorted wave Born approximation (DWBA) calculation based on a doubly closed $1p$ shell. Harmonic oscillator orbitals, with $b=1.77$ fm chosen to fit the ^{16}O root mean square (rms) charge radius 2.27 fm (Ref. 12), yield a remarkably good fit to the data in Fig. 5. The center-of-mass and nucleon form factors are included in the calculated form factor. The harmonic-oscillator curve in Fig. 5 is not significantly altered by recent shell model calculations of the ^{16}O ground state. The model space of Amos *et al.*[38] includes 2p2h configurations spanning the $1s_{1/2}$ to $2p\,1f$ shells. The "ZBM" model space of Ref. 39 includes up to 4p4h configurations, limited to the $1p_{1/2}$, $1d_{5/2}$, and $2s_{1/2}$ orbitals. Both calculations depopulate the $1p$ shell by less than one nucleon. Consequently, the radial scale required to fit the experimental charge radius is not significantly altered from the closed $1p$-shell result.

In Refs. 40 and 41 the elastic magnetic electron scattering data from ^{17}O of Hynes *et al.*[42] were fitted in the single-particle model by adjusting the shell-model potential parameters for the $1d_{5/2}$ orbit and adjusting the strength of each multipole. Woods-Saxon (WS) potential parameters obtained in this way are listed in Table V and Ref. 43. These Woods-Saxon parameters yield an ^{16}O rms charge radius of only 2.67 rm, and shift the minimum in the DWBA ^{16}O elastic form factor to 1.75 fm^{-1} (Fig. 5). The $1d_{5/2}$ orbit obtained from Table V is similar to the orbit obtained by Cooper[44] from an analysis of (d,p) reactions. This $1d_{5/2}$ orbit is also in good agreement with a self-consistent renormalized Brueckner calculation of

TABLE IV. Ratios of (e,e') form factors squared. The "(e,e') data" column is the weighted average of the (e,e') data.

State (MeV)	(e,e') data	$(\pi^{\pm},\pi^{\pm'})$ analysis		
		Δ dominance	DWIA	Δ hole
$\frac{17.79}{18.98}$	0.037±0.001	0.049±0.018	0.050±0.019	0.058±0.022
$\frac{19.80}{18.98}$	$\leq 10^{-3}$[a]	$(5.8\pm9.4)\times10^{-4}$	$(2.6\pm6.5)\times10^{-4}$	$(0.6\pm3.5)\times10^{-4}$

[a]One standard deviation statistical upper bound.

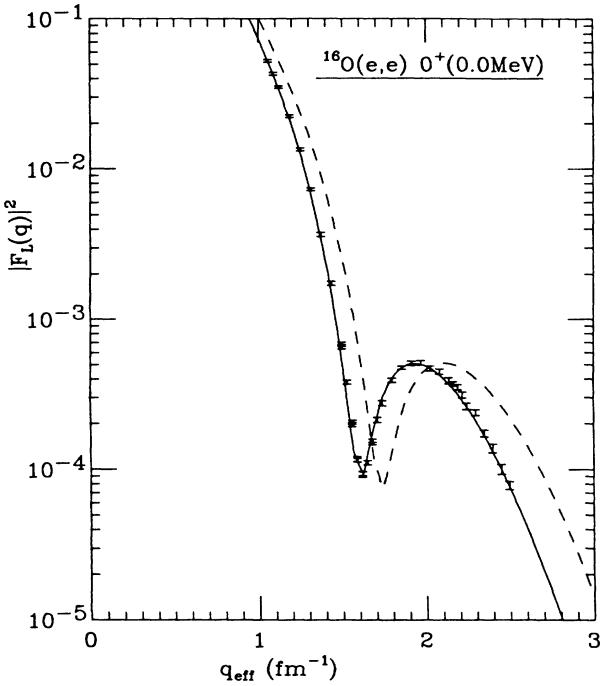

FIG. 5. ^{16}O elastic electron scattering form factor squared. The data are the 375 MeV data from Ref. 37. The curves are calculated in distorted-wave Born approximation from a doubly closed $(1s \oplus 1p)$-shell density. The solid curve is a harmonic oscillator density, with $b=1.77$ fm. The dashed curve is a Woods-Saxon (WS) density, with parameters from Table V.

^{16,17}O performed by Vary *et al.*[45] in a large basis. Thus the $1d_{5/2}$ orbit of Table V is motivated by both phenomenology and theory.

B. Meson exchange currents

As noted in Fig. 2, the form factor of the 18.98 MeV state has a smaller radial scale than implied by the ^{16}O ground state. The oscillator model fits in Fig. 2 are parametrizations of the data. In order to draw specific conclusions about the one-body transition densities, we need to include the effects of possible two-body currents such as meson-exchange currents (MEC's). MEC calculations of Dubach[33,46] include virtual pion, nucleon-antinucleon pair, and isobar terms. The pair term is generally the largest. MEC calculations for 4^- states in ^{16}O are also discussed in Ref. 47. In Figs. 6(a) and 6(b) we compare the MEC calculation with the data for the 18.98 MeV $T=1$ state. In Fig. 6 the meson-exchange currents are added to the isovector form factor and then scaled by the isovector amplitude Z_1. In Fig. 6(a) the calculations use harmonic oscillator wave functions with $b=1.75$ fm. A normalization factor $Z_1^2=0.56$ gives the best fit to the data. The fit is unaffected by the two data points with $q<1.0$ fm^{-1}. The calculation is a poor representation of the data, consistently overshooting on the low-q side and undershooting on the high-q side of the form factor maximum. In Fig. 6(b) the harmonic-oscillator ($b=1.75$ fm) meson-exchange currents are added to the Woods-Saxon 1p1h density to obtain the total form factor.

The MEC's enhance the form factor by approximately 10% in the vicinity of the maximum. Thus inclusion of the MEC systematically suppresses extracted spectroscopic amplitudes by the same factor. However, in the WS + MEC fit of Fig. 6(b), the extracted amplitude is not suppressed relative to the harmonic oscillator fit of Fig. 2. The calculated Woods-Saxon form factor is slightly shifted to lower q relative to the data in Fig. 6(b). The fit compensates by augmenting the amplitude. The spectro-

TABLE V. Woods-Saxon potential parameters. E_{nlj} are binding energies.

$$V(r)=-\left[V_0+V_S\left[\frac{1}{m_\pi c}\right]^2\mathbf{L}\cdot\boldsymbol{\sigma}\frac{1}{r}\frac{\partial}{\partial r}\right]f(r)$$
$$f(r)=(1+e^{(r-R)/a})^{-1}$$

	$V_0=53.07$ MeV $R=3.0$ fm	$V_S=7.14$ MeV $a=0.6$ fm
Orbit	E_{nlj}(neutron) (MeV)	E_{nlj}(proton) (MeV)
$1d_{5/2}$	4.11	0.85
$1p_{3/2}$	17.68	13.88

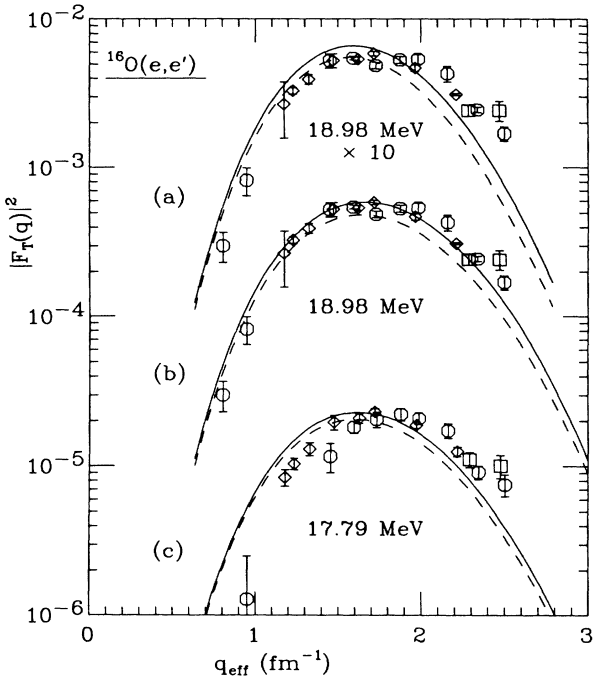

FIG. 6. ^{16}O $1\hbar\omega$ + meson exchange current (MEC) $M4$ form factors compared to (e,e') data. Dashed lines: Single particle form factor. Solid lines: MEC (Ref. 33) included. (a) 18.98 MeV, single-particle harmonic-oscillator calculation times 0.56, with $b=1.75$ fm. The data and curves are multiplied by 10. (b) 18.98 MeV, single-particle Woods-Saxon calculation times 0.42, WS parameters of Table V. (c) 17.79 MeV, single particle Woods-Saxon calculation, spectroscopic amplitudes of Table III, DWIA.

scopic amplitudes obtained for the 18.98 MeV state in Fig. 2 (pure harmonic oscillator) and Fig. 6(b) (WS + MEC) are $0.63+0.01$ and $0.65+0.01$, respectively, but the χ^2 per degree of freedom are 2.4 and 3.8, respectively.

The Woods-Saxon form factor of the 17.79 MeV state is plotted in Fig. 6(c). The isospin amplitudes are taken from Table III, heading DWIA. The meson-exchange currents are included in the isovector component of the form factor only. The WS form factor is a poor representation of the 17.79 MeV state. In Fig. 7 we plot the ratio of the form factors for the 17.79 and 18.98 MeV levels. The data are consistent with a constant ratio, though there is an approximately one-standard-deviation tendency for the ratio to increase with momentum transfer. This trend is curious, since there are several effects which could give the ratio a small negative (rather than positive) slope. The calculated MEC's (Ref. 33) enhance the $T=1$ form factor and not the $T=0$ form factor. The isoscalar WS form factor is suppressed at high q (relative to the isovector WS form factor) by the enhancement at high q of the neutron contribution (relative to the proton contribution) to the Woods-Saxon single particle form factor. Both the isovector MEC and the Coulomb splitting of the neutron and proton orbits tend to enhance the calculated high q, $T=1$ form factor over the $T=0$ form factor. Isospin mixing in the 17.79 MeV states reduces but does not eliminate these effects.

In Fig. 7 we plot the calculated form factor ratio, based on the isospin amplitudes of Table III. The uncertainties in the isospin amplitudes for the 17.79 and 18.98 MeV states imply an uncertainty of approximately 40% in the calculated ratios plotted in Fig. 7. However, this systematic uncertainty is independent of q. The displayed curves are calculated both with and without MEC's and for both harmonic oscillator and Woods-Saxon wave functions. All of the calculations predict large (factors of 2 or more) effects at $q\approx 3.5$ fm^{-1}. In this region, both the Woods-Saxon and MEC form factors change sign, and the harmonic-oscillator form factor falls well below the contribution of the MEC. The Woods-Saxon orbitals were computed with the parameters of Table V, including the Coulomb potential for the protons.

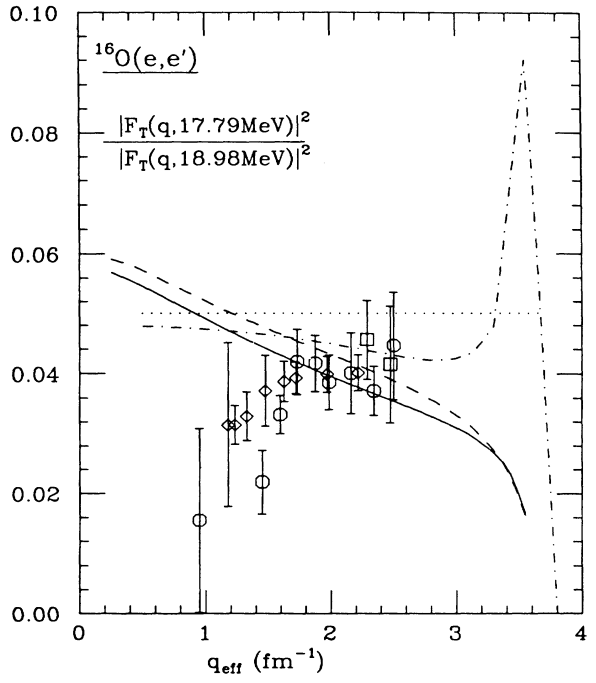

FIG. 7. Ratio of form factors squared for the 17.79 and 18.98 MeV states. The curves are calculated from the spectroscopic amplitudes of Table III, DWIA. Dotted line, harmonic oscillator; dotted-dashed, harmonic oscillator + MEC; dashed; Woods-Saxon; Solid, Woods-Saxon + MEC.

V. CONCLUSONS

The ratios of the electron scattering form factors of 4^- states at 17.79, 18.98, and 19.80 MeV are consistent with the analyses of $\pi^{\pm}$ asymmetries for the same states. The electron scattering data also provide a calibration of the absolute accuracy of the DWIA (π,π') calculation described in Ref. 8. The (e,e') form factors are strongly affected by the isospin mixing implied by the pion scattering data. The total isovector and isoscalar $M4$ strengths observed are 41% and 23%, respectively, of the pure single particle values.

The form factors are strongly enhanced at high q compared to the shape expected for a $d_{5/2}$ orbital within the oscillator model of ^{16}O for a closed-shell ground state. On the other hand, the empirical isovector form factor is in good agreement with a MEC plus Woods-Saxon calculation based on WS orbitals fit to the elastic $M5$ multipole of ^{17}O. However, the combination of meson exchange currents and neutron-proton differences in the WS orbitals introduces a disparity between the calculated isoscalar and isovector form factors at high q, which is contradicted by the data (Fig. 7). It remains an open question whether the isospin-independent enhancement observed in the data at high q is due to the participation of shells beyond the $2s\,1d$ shell, changes in the single particle orbits, modifications to the one body current operator, including MEC and relativistic effects, or all of the above.

Abnormal-parity states are identified at 17.88, 18.63, and 20.51 MeV. The form factors of these states suggest 4^- assignments. A comparison of (e,e'), (p,p'), and (π,π') spectra indicates that these states must be isovector, if they are 4^-. The contribution of these three states increases the net isovector strength observed to 52% of a $1\hbar\omega$ model.

ACKNOWLEDGMENTS

We wish to thank Prof. J. Dubach for making his shell model and MEC calculations available to us. We thank Dr. T. Karapiperis for helpful discussions of the Δ-hole model. We also thank Prof. D. M. Manley for many helpful comments on the manuscript. One of us (R.W.L.) would like to acknowledge the support of the Fannie and John Hertz Foundation. This work was supported in part by the National Science Foundation and the United States Department of Energy under Contracts DE-AC02-76ER03069 and DE-FG05-ER40285.

[a]Present address: Department of Physics, University of Washington, Seattle, WA 98195.
[b]Present address: Harris Semiconductor, MS 51-180, Melbourne, FL 32901.
[c]Present address: Department of Physics, College of William and Mary, Williamsburg, VA 23189.
[d]Present address: Department of Physics, University of New Hampshire, Durham, NH 03824.
[e]Present address: Los Alamos National Laboratory, MS D-406, Los Alamos, NM 87544.
[f]Present address: Department of Physics, University of Kentucky, Lexington, KY 40506.
[g]Present address: Department of Physics and Astronomy, University of Maryland, College Park, MD 20742.
[h]Present address: Department of Physics, Tel-Aviv University, Ramat-Aviv, Tel-Aviv, Israel.
[i]Present address: Department of Physics, University of Virginia, Charlottesville, VA 22901.
[j]Present address: Supercomputer Computations Research Institute, Florida State University, Tallahassee, FL 32306.

[1]I. Sick, E. B. Hughes, T. W. Donnelly, J. D. Walecka, and G. E. Walker, Phys. Rev. Lett. **23**, 1117 (1969).
[2]G. Mairle, G. J. Wagner, P. Doll, K. T. Knöpfle, and H. Breuer, Nucl. Phys. **A299**, 39 (1978).
[3]R. S. Henderson, B. M. Spicer, I. D. Svalbe, V. C. Officer, G. G. Shute, D. W. Devins, D. L. Friesel, W. P. Jones and A. C. Attard, Aust. J. Phys. **32**, 411 (1979).
[4]D. B. Holtkamp, W. J. Braithwaite, W. Cottingame, S. J. Greene, R. J. Joseph, C. Fred Moore, C. L. Morris, J. Piffaretti, E. R. Siciliano, H. A. Thiessen, and D. Dehnhard, Phys. Rev. Lett. **45**, 420 (1980).
[5]W. Bertozzi, Nucl. Phys. **A374**, 109c (1982).
[6]F. Petrovich, W. G. Love, A. Picklesimer, G. E. Walker, and E. R. Siciliano, Phys. Lett. **95B**, 166 (1980).
[7]F. Petrovich and W. G. Love, Nucl. Phys. **A354**, 499c (1981).
[8]J. A. Carr, F. Petrovich, D. Halderson, D. B. Holtkamp, and W. B. Cottingame, Phys. Rev. C **27**, 1636 (1983).
[9]T. Karapiperis and E. J. Moniz, Phys. Lett. **148B**, 253 (1984).
[10]T. DeForest and J. D. Walecka, Adv. Phys. **15**, 1 (1966).
[11]G. R. Hammerstein, R. H. Howell, and F. Petrovich, Nucl. Phys. **A213**, 45 (1973).
[12]H. Miska, B. Norum, M. V. Hynes, W. Bertozzi, S. Kowalski, F. N. Rad, C. P. Sargent, T. Sasanuma, and B. L. Berman, Phys. Lett. **83B**, 165 (1979).
[13]W. Bertozzi, M. V. Hynes, C. P. Sargent, W. Turchinetz, and C. Williamson, Nucl. Instrum. Methods **162**, 211 (1979).
[14]W. Bertozzi, M. V. Hynes, C. P. Sargent, C. Creswell, P. C. Dunn, A. Hirsch, M. Leitch, B. Norum, F. N. Rad, and T. Sasanuma, Nucl. Instrum. Methods **141**, 457 (1977).
[15]J. J. Kelly, computer code ALLFIT (unpublished).
[16]T. N. Buti, J. Kelly, W. Bertozzi, J. M. Finn, F. W. Hersman, C. Hyde-Wright, M. V. Hynes, M. A. Kovash, S. Kowalski, R. W. Lourie, B. Murdock, B. E. Norum, B. Pugh, C. P. Sargent, and W. Turchinetz, Phys. Rev. C **33**, 755 (1986).
[17]G. J. Vanpraet and W. C. Barber, Nucl. Phys. **79**, 550 (1969).
[18]T. E. Drake, E. L. Tomusiak, and H. S. Caplan, Nucl. Phys. **A118**, 138 (1968).
[19]A. Goldmann and M. Stroetzel, Phys. Lett. **31B**, 287 (1970).
[20]M. Stroetzel and A. Goldman, Z. Phys. **233**, 245 (1970).
[21]A. Hotta, K. Itoh, and T. Saito, Phys. Rev. Lett. **33**, 790 (1974).
[22]R. D. Graves, B. A. Lamers, Anton Nagl, H. Überall, V. Devanthan, and P. R. Subramanian, Can. J. Phys. **58**, 48 (1980).
[23]G. Küchler, A. Richter, E. Spamer, and W. Steffen, and W. Knüpfer, Nucl. Phys. **A406**, 473 (1983).
[24]K. W. Kemper, G. G. Shute, C. H. Atwood, L. K. Fifield, and T. R. Ophel, Nucl. Phys. **A405**, 348 (1983).
[25]H. Nann, A. D. Bacher, G. T. Emery, D. L. Friesel, W. P. Jones, and C. Olmer, IUCF Annual Report, 1980.
[26]J. J. Hamill, R. J. Peterson, and M. Yasue, Nucl. Phys. **A408**, 21 (1983).
[27]F. Ajzenberg-Selove, Nucl. Phys. **A375**, 21 (1982).
[28]C. E. Hyde-Wright, Ph.D. thesis, Massachusetts Institute of Technology, 1984.
[29]J. J. Kelly, Ph.D. thesis, Massachusetts Institute of Technology, 1981; C. Hyde-Wright, W. Bertozzi, T. N. Buti, J. M. Finn, M. A. Kovash, R. Lourie, B. Murdock, B. Pugh, P. Ulmer, B. L. Berman, F. W. Hersman, M. V. Hynes, J. J. Kelly, B. Norum, A. D. Bacher, G. T. Emery, C. C. Foster, W. P. Jones, and D. W. Miller, Bull. Am. Phys. Soc. **27**, 691 (1983); J. M. Finn, W. Bertozzi, T. Buti, F. W. Hersman, C. Hyde, M. A. Kovash, V. Murdock, B. Pugh, P. Ulmer, M. V. Hynes, J. J. Kelly, A. D. Bacher, G. T. Emery, C. C. Foster, W. P. Jones, D. W. Miller, and B. L. Berman, *ibid.* **27**, 664 (1983).
[30]See AIP Document No. 35-880-6 for six pages of (e,e′) cross section data for the states at 17.79, 17.88, 18.63, 18.98, 19.80, and 20.51 MeV. Order by PAPS number and journal reference from American Institute of Physics, Physics Auxiliary Publication Service, 335 E. 45th St., New York, NY 10017. The price is $1.50 for microfiche or $5.00 for photocopies. Airmail additional. Make checks payable to the American Institute of Physics.
[31]F. Petrovich, C. H. Poppe, S. M. Austin, and G. M. Crawley, Nucl. Phys. **A383**, 355 (1982).
[32]D. B. Holtamp, S. J. Seestrom-Morris, D. Dehnhard, H. W. Baer, C. L. Morris, S. J. Greene, C. J. Harvey, D. Kurath, and J. A. Carr, Phys. Rev. C **31**, 957 (1985).
[33]J. Dubach, private communication.
[34]S. Cohen and D. Kurath, Nucl. Phys. **73**, 1 (1965).
[35]T. T. S. Kuo and G. E. Brown, Nucl. Phys. **85**, 40 (1966).
[36]D. J. Millener and D. Kurath, Nucl. Phys. **A255**, 315 (1975).
[37]I. Sick and J. S. McCarthy, Nucl. Phys. **A150**, 631 (1970).
[38]K. Amos, W. Bauhoff, I. Morrison, S. F. Collins, R. S. Henderson, B. M. Spicer, G. C. Shute, V. C. Officer, D. W. Devins, D. L. Friesel, and W. P. Jones, Nucl. Phys. **A413**, 255 (1984).
[39]K. A. Snover, E. G. Adelberger, P. G. Ikossi, and B. A. Brown, Phys. Rev. C **27**, 1837 (1983); B. A. Brown, private communication.
[40]R. S. Hicks, Phys. Rev. C **25**, 695 (1982).
[41]S. Burzynski, M. Baumgartner, H. P. Gubler, J. Jourdan, H. O. Meyer, G. R. Plattner, H. W. Roser, and I. Sick, Nucl. Phys. **A399**, 230 (1980).
[42]M. V. Hynes, H. Miska, B. Norum, W. Bertozzi, S. Kowalski, F. N. Rad, C. P. Sargent, T. Sasanuma, W. Turchinetz, and B. L. Berman, Phys. Rev. Lett. **42**, 1444 (1979).
[43]T. W. Donnelly and I. Sick, Rev. Mod. Phys. **56**, 561 (1984).
[44]M. D. Cooper, W. F. Hornyak, and P. G. Roos, Nucl. Phys. **A218**, 249 (1974).
[45]J. P. Vary, R. H. Belehard, and R. J. McCarthy, Phys. Rev. C **21**, 1626 (1980).
[46]J. Dubach, J. H. Koch, and T. W. Donnelly, Nucl. Phys. **A271**, 279 (1976); E. L. Tomusiak, M. Kimura, J. L. Friar, B. F. Gibson, G. L. Payne, and J. Dubach, Phys. Rev. C **32**, 2075 (1985).
[47]J. S. Dehesa, S. Krewald, A. Lallena, and T. W. Donnelly, Nucl. Phys. **A436**, 573 (1985); S. Krewald, A. M. Lallena, and J. S. Dehesa, *ibid.* **A448**, 685 (1986); A. M. Lallena, J. S. Dehesa, and S. Krewald, Phys. Lett. **146B**, 294 (1984).